

FEM model for reinforced concrete frames loaded by seismic forces

Dušan Kovačević *

Abstract

Objective of the presented research is the formulation of one enough sophisticated and, for engineering practice, convenient finite element method (FEM) based numerical model for reinforced concrete frames loaded by seismic actions. For modeling of concrete and steel nonlinear behavior uniaxial constitutive rules are applied. The proposal for inclusion the frame joint deterioration, as well as, interaction of shear and flexural forces (inclined cracks effects), in this model, is given additionally. The results of few numerical tests (linear/nonlinear analysis of reinforced concrete frame loaded by three seismic actions) are given as an illustration of presented theoretical research.

Keywords: numerical modeling, nonlinear analysis, reinforced concrete frame, seismic action

1 Introduction

Structural modeling is the process of creation of idealized and simplified representation of structural behavior and it is an essential step in structural analysis and design. Errors and inadequacies in modeling may

*Faculty of Technical Sciences, Civil Engineering Department, University of Novi Sad, Serbia and Montenegro, e-mail: dusan@uns.ns.ac.yu

cause serious design defects and difficulties. Numerical modeling is a mathematical realization of selected structural modeling concept.

Particularly, the main goal of structural modeling is to adopt the “optimal” model - compromise between complexity and quality of approximation. The optimal model should provide a sufficient reliability in prediction of the “real” structural behavior (quality of approximation), with complexity corresponds to the actual computation capabilities (method of numerical analysis, computer technology, system and applicative software development level, etc.). Numerical model quality can be determined by the overall structural behavior modeling ability, not only according “local” effects modeling ability.

Due to numerical efficiency and simple software implementation, FEM has become a fundamental method of a structural analysis and numerical modeling of structural behavior. One classification of numerical models for reinforced concrete (RC), could be formulated by three model groups, Fig. 1:

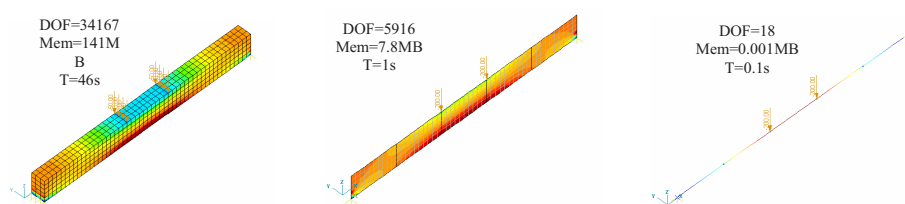


Figure 1: Different numerical model for the same structural element (simple supported beam)

- 3D (3-dimensional, solid) finite element FE models enable the highest quality of approximation, but model complexity and difficulties in its application (computation costs, in the first place) make difficult the structural analysis of the real buildings. Therefore, 3D FE models can be adopted as benchmark-test models, for verification of simpler (2D or 1D) models.
- 2D (membrane, plate, shell) FE models are frequently used in numerical analysis of RC beams, especially for the research of so-called local effects (“aggregate interlock”, “dowel action”, etc.).

Basic advantage in comparison to models with beam FE lays in a possibility of modeling the shear stresses influence in RC elements behavior.

- 1D (beam) FE models are the simplest and make possible non-linear analysis in everyday engineering practice, but not only in the phase of preliminary design. Nevertheless, application of the 2D beam FE enables the results that confirm adequate quality of approximation. Experimental research of many authors indicates that.

2 Model with 2D beam FE

Beam FE can be classified into two basic groups:

- 1D beam FE - the shear deformations are neglected (Bernoulli-Navier's beam theory), and
- 2D beam FE - influence of the shear is taken into account (Timoshenko's beam theory).

A criterion for a determination of model dimensionality is a number of parameters that define displacement field of the beam FE. In the case of 1D beam FE a rotation of the cross-section are determined as corresponding derivations of displacement, while in the case of 2D beam FE those two parameters are independent.

The type of discretization could also define dimensionality of a model. In the nonlinear analysis, by application of a beam FE, discretization is usually performed both along the length of the structural element and the height of the cross-section. This circumstance indicates the physical/geometrical two-dimensionality of the problem. All further considerations will be based upon the, in that sense, twodimensional beam FE.

3 Basic suppositions, geometry and coordinates

In formulation of the model with 2D beam FE the suppositions are following:

- Straight, plane, two-joint beam FE approximates a RC element (beam, column). Two displacements and one rotation per joint are the degrees of freedom (DOF). Beam FE cross-section is divided in certain number of finite thickness concrete and steel layers (concrete or steel, area A_i , tangent modulus E_i). Behavior of these layers under the cyclic loading is modeled by corresponding uniaxial constitutive rules. Beam FE geometry in a local and global coordinate system is shown in Fig. 1.

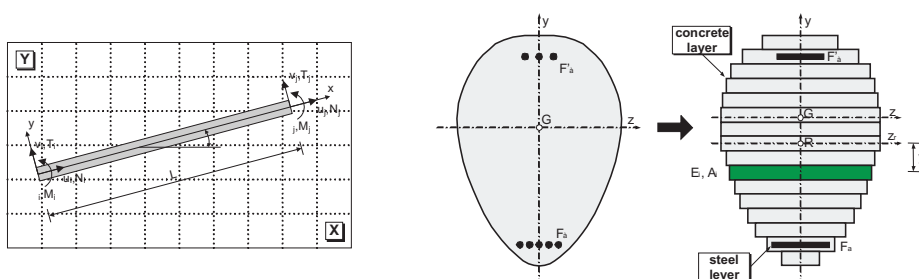


Figure 2: Beam FE DOF and finite layers discretization of a beam FE cross-section

- The uniform cracks distribution (so-called “smeared cracks approach”) is accepted in zones where concrete tension strength is reached.
- Linear strain distribution is adopted along the height of the cross-section, because of negligible shear influence in the total deformation field for the common beam. Additionally, in this way, the so-called “shear locking” effect (overestimated the participation of shear deformation in the total deformation energy) is avoid. Namely, model with unreal high stiffness is obtained, if 2D beam FE with rotation field independent from displacement field is applied. This effect is particularly evident in elements with high

length/height ratio and elements characterized with lower level of interpolation (beam with two joints, for example). In contrast to shear in strict sense, axial and shear stresses interaction influence, as a cause of inclined cracks appearance must be included in model, what is discussed later.

- Concrete-reinforcement interaction (bond) is modeled implicitly by so-called “tension stiffening effect”.
- Third degree L’Hermite polynomials are adopted for the interpolation of beam flexural displacements and rotations and first degree polynomials are adopted for approximation of beam longitudinal displacements.
- External loading is applied in beam FE joints, regardless to real load configuration.

4 Interpolation functions

In nonlinear analysis (large displacements, large strains and material nonlinearity), usually is applied incremental form of equilibrium i.e. increments of displacements are the basic unknowns. In formulation of incremental relations for the beam FE it is started from the nonlinear differential equation that defines a relation between the strain and displacements function:

$$\varepsilon_x = \frac{du(x)}{dx} + \frac{1}{2} \left[\left(\frac{du(x)}{dx} \right)^2 + \left(\frac{dv(x)}{dx} \right)^2 + \left(\frac{dw(x)}{dx} \right)^2 \right] \quad (1)$$

For the plane beam, the member $(dw(x)/dx)^2$ have a zero value and the member $(du(x)/dx)^2$ can be neglected because of its small contribution to overall strain ε_x . Eq. (1) now obtains the form:

$$\varepsilon_x = \varepsilon_{xL} + \varepsilon_{xN} = \frac{du(x)}{dx} + \frac{1}{2} \left(\frac{dv(x)}{dx} \right)^2 \quad (2)$$

The members $du(x)/dx$ and $(dv(x)/dx)^2$ represents a linear part and a nonlinear part of the total strain ε_x . The linear member is the function of coordinates for each point $P(x_p, y_p)$ of the FE. According to the bending theory:

$$\varepsilon_{xL}(x, y) = \frac{du(x)}{dx} = \frac{du_s(x)}{dx} - y \frac{d^2v(x)}{dx^2}. \quad (3)$$

Here, functions $u_s(x)$ and $v(x)$ define the longitudinal and transversal component of displacements. Based on the (2) and (3), the equation that defines the total strain in an arbitrary beam's point becomes:

$$\varepsilon_x(x, y) = \frac{du_s(x)}{dx} - y \frac{d^2v(x)}{dx^2} + \frac{1}{2} \left(\frac{dv(x)}{dx} \right)^2 \quad (4)$$

Third degree polynomial as the interpolation function ensures the fulfillment of a compatibility conditions between beam FE joints (C^0 continuity of the function and C^1 continuity of first derivative). Functions $u_s(x)$ and $v(x)$, expressed by interpolation polynomials and the vector of FE joint displacements \mathbf{u} , are:

$$u_s(x) = [N_1 \ 0 \ 0 \ N_4 \ 0 \ 0] \cdot \mathbf{u}, \quad (5)$$

$$v(x) = [0 \ N_2 \ N_3 \ 0 \ N_5 \ N_6] \cdot \mathbf{u}, \quad (6)$$

where are

N_1, N_2 - linear interpolation functions,

$N_2, N_3, \dots, N_5, N_6$ - third degree L'Hermite's polynomial interpolation functions,

L - beam span and

$\mathbf{u}^T = \{u_i, v_i, \varphi_i, u_j, v_j, \varphi_j\}$ - joint displacement vector.

The first and second derivatives of displacements are:

$$\frac{du_s(x)}{dx} = \left[\frac{dN_1}{dx} \ 0 \ 0 \ \frac{dN_4}{dx} \ 0 \ 0 \right] \cdot \mathbf{u} \equiv \mathbf{G}_S \cdot \mathbf{u}, \quad (7)$$

$$\frac{dv(x)}{dx} = \left[0 \ \frac{dN_2}{dx} \ \frac{dN_3}{dx} \ 0 \ \frac{dN_5}{dx} \ \frac{dN_6}{dx} \right] \cdot \mathbf{u} \equiv \mathbf{G}_B \cdot \mathbf{u}, \quad (8)$$

$$\frac{d^2v(x)}{dx^2} = \left[0 \quad \frac{d^2N_2}{dx^2} \quad \frac{d^2N_3}{dx^2} \quad 0 \quad \frac{d^2N_5}{dx^2} \quad \frac{d^2N_6}{dx^2} \right] \cdot \mathbf{u} \equiv \mathbf{B}_B \cdot \mathbf{u}. \quad (9)$$

Thus, the equation for a total strain is:

$$\varepsilon_x(x, y) = \mathbf{G}_S \cdot \mathbf{u} - y\mathbf{B}_B \cdot \mathbf{u} + \frac{1}{2}\mathbf{u}^T \cdot (\mathbf{G}^T \otimes \mathbf{G}) \cdot \mathbf{u}, \quad (10)$$

or, in a shorter way:

$$\varepsilon_x(x, y) = \mathbf{B} \cdot \mathbf{u} + \frac{1}{2}\mathbf{u}^T \cdot (\mathbf{G}^T \otimes \mathbf{G}) \cdot \mathbf{u}, \quad (11)$$

where $\mathbf{B} = \mathbf{G}_S - y\mathbf{B}_B$ and $\mathbf{G} = \mathbf{G}_B$ (corresponding to large and small displacements).

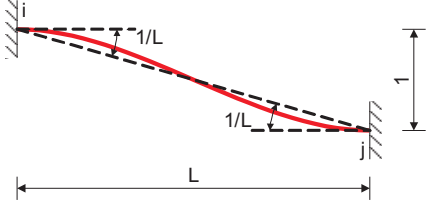
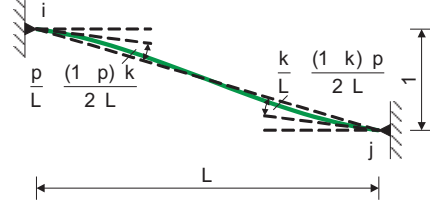
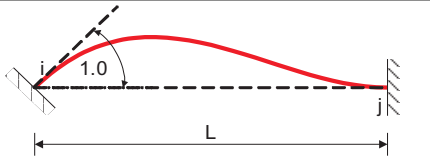
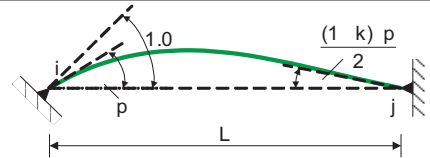
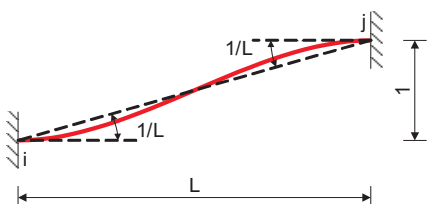
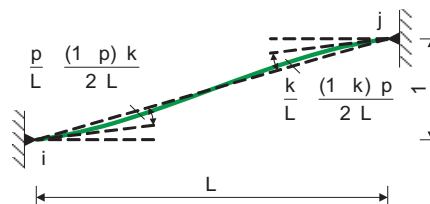
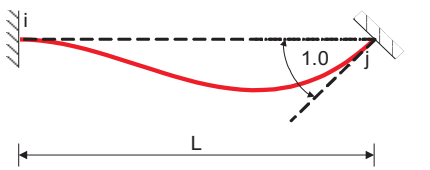
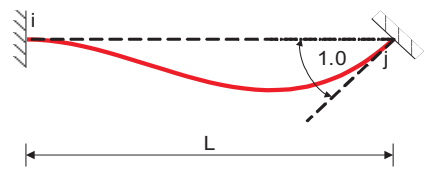
In RC structures, because of joint deterioration due to load progress, the rotations of the beam ends cross sections and joint rotations are not compatible in general (the connections are neither rigid nor hinge). There are few possibilities to involve the influence of rotational joint deterioration in a structural analysis. One approach takes the ratio "beam-end-rotation/joint-rotation" (i.e. ϕ^*/ϕ) as a "rate" of rotational deterioration. These quotients could be regarded as "fixing degree" (FD). Their values vary from "0" to "1" (from pinned to rigid connection). For the start and end member joint FD are:

$$p = \frac{\varphi_i^*}{\varphi_i} \quad \text{and} \quad k = \frac{\varphi_j^*}{\varphi_j}. \quad (12)$$

Table 1 explains interpolation functions for beam FE with fully rigid (N_2, N_3, N_5, N_6) and partially rigid ends ($N_2^*, N_3^*, N_5^*, N_6^*$). Linear functions are used for defining the longitudinal displacements $N_1 = 1 - x/L$ and $N_4 = x/L$ while fields of transversal and longitudinal displacements are assumed independent.

Zero value of coefficients "p" and "k" is related to ideal hinged beam end connection, while their "1.0" value corresponds to ideal rigid connection. By varying the values of coefficients "p" and "k" ($0 \leq p \leq 1$ and $0 \leq k \leq 1$), all the beam "types" could be modeled (pinned connection, rigid connection or connection of arbitrary FD on one or both ends).

Table 1: Interpolation functions for for beam FE with fully rigid and partially rigid ends

fully rigid ends	partially rigid ends
	
$N_2 = 1 - 3\left(\frac{x}{L}\right)^2 + 2\left(\frac{x}{L}\right)^3$	$N_2^* = \left(\frac{p}{L} - \frac{(1-p)k}{2L}\right) N_3 + \left(\frac{k}{L} - \frac{(1-k)p}{2L}\right) N_6 + 1 - \frac{x}{L}e$
	
$N_3 = x\left(1 - \frac{x}{L}\right)^2$	$N_3^* = pN_3 - \frac{(1-k)p}{2}N_6$
	
$N_5 = 3\left(\frac{x}{L}\right)^2 - 2\left(\frac{x}{L}\right)^3$	$N_5^* = \left(\frac{(1-p)k}{2L} - \frac{p}{L}\right) N_3 + \left(\frac{(1-k)p}{2L} - \frac{k}{L}\right) N_6 + \frac{x}{L}$
	
$N_6 = \frac{x^2}{L}\left(\frac{x}{L} - 1\right)$	$N_6^* = kN_6 - \frac{(1-p)k}{2}N_3$

5 Incremental equilibrium equation of the beam FE

Equilibrium conditions in the incremental form can be obtained by the so-called Lagrange formulation by the adoption of displacement increments as unknowns.

FE state can be analyzed in three configurations: “Start” - “S”, “Current” - “C” and “Next” - “N”, at incrementally small distance from the current one, Fig. 3. If the “C” configuration is adopted as the referent one, it is “updated Lagrange formulation”. Application of this formulation demands a permanent update of FE local coordinate system.

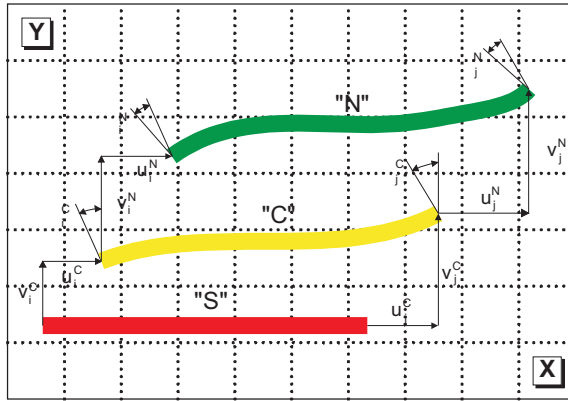


Figure 3: “Start”, “Current” and “Next” incremental configuration

The incremental variant of the Eq. (11), for the current configuration, is:

$$\Delta \varepsilon_x(x, y) = \mathbf{B} \cdot \Delta \mathbf{u} + \frac{1}{2} \Delta \mathbf{u}^T \cdot \mathbf{G}^T \cdot \mathbf{G} \cdot \Delta \mathbf{u}. \quad (13)$$

Well-known equilibrium condition in tangent form is:

$$d\mathbf{r} = \int_V \mathbf{B}^T E_t \mathbf{B} \cdot d\mathbf{u} dV + \int_V \mathbf{G}^T \sigma \mathbf{G} \cdot d\mathbf{u} dV \quad (14)$$

or:

$$d\mathbf{r} = \mathbf{k}_L \cdot d\mathbf{u} + \mathbf{k}_{NL} \cdot d\mathbf{u} \equiv \mathbf{k}_t \cdot d\mathbf{u}, \quad (15)$$

where are:

$$\begin{aligned} \mathbf{k}_t &= \mathbf{k}_L + \mathbf{k}_{NL} - \text{tangent stiffness matrix,} \\ \mathbf{k}_L &= \int_V E_t \mathbf{B}^T \otimes \mathbf{B} dV - \text{elastic-plastic stiffness matrix,} \\ \mathbf{k}_{NL} &= \int_V \sigma \mathbf{G}^T \otimes \mathbf{G} dV - \text{geometrical stiffness matrix and} \\ &E_t - \text{tangent modulus.} \end{aligned}$$

The Eq. (15) represents the equilibrium condition of the finite element in the local coordination system, in a tangent form. Effects of material nonlinearity are modeled by elastic-plastic stiffness matrix k_L . Effects of geometrical nonlinearity (large displacements and small strains) are modeled by geometrical stiffness matrix k_{NL} . Errors in modeling of large rotations are reduced indirectly, due to discretization of beams by number of FE.

6 Tangent stiffness matrix of 2D beam FE

Coefficients of matrices are determined based on the Eq. (13). If the relation $\mathbf{B} = \mathbf{G}_S - y\mathbf{B}_B$ is included in the first member of this equation, it is obtained:

$$\mathbf{B} = \begin{bmatrix} \frac{dN_1}{dx} & -y \frac{d^2 N_2}{dx^2} & -y \frac{d^2 N_3}{dx^2} & \frac{dN_4}{dx} & -y \frac{d^2 N_5}{dx^2} & -y \frac{d^2 N_6}{dx^2} \end{bmatrix}. \quad (16)$$

If the average value is adopted for the elasticity modulus along the overall length of the element in one layer, the first member in Eq. (13) can be written in the form:

$$\mathbf{k}_L = \int_A E_t dA \int_L \mathbf{B}^T \otimes \mathbf{B} dx \quad (17)$$

Integration along the FE length is performed analytically, thus obtaining the beam FE stiffness matrix:

$$\mathbf{k}_L = \begin{bmatrix} \mathbf{k}_{L,11} & \mathbf{k}_{L,12} \\ sym & \mathbf{k}_{L,22} \end{bmatrix}, \quad (18)$$

where

$$\mathbf{k}_{L,11} \equiv \begin{bmatrix} \frac{EF}{L} & 0 & \frac{ES}{L} \frac{p}{2} (3-k) \\ \frac{3EI}{L^3} (p+k+2kp) & \frac{3EI}{L^2} p(1+k) & \\ \frac{EI}{L} p(3+k) & & \end{bmatrix},$$

$$\mathbf{k}_{L,12} \equiv \begin{bmatrix} -\frac{EF}{L} & 0 & \frac{ES}{L} \frac{k}{2} (p-3) \\ 0 & -\frac{3EI}{L^3} (p+k+2kp) & \frac{3EI}{L^2} k(1+p) \\ \frac{ES}{L} \frac{p}{2} (k-3) & -\frac{3EI}{L^2} p(1+k) & \frac{2EI}{L} pk \end{bmatrix},$$

$$\mathbf{k}_{L,12} \equiv \begin{bmatrix} \frac{EF}{L} & 0 & \frac{ES}{L} \frac{k}{2} (3-p) \\ \frac{3EI}{L^3} (p+k+2kp) & -\frac{3EI}{L^2} k(1+p) & \\ \frac{EI}{L} k(3+p) & & \end{bmatrix}.$$

Value “S” is the cross-section moment of area related to the reference axis. This term introduces the cross-section centroid change due to change of stiffness along the cross-section height.

Geometrical stiffness matrix \mathbf{k}_{NL} is obtained by means of the Eq. (8) and the second member in the Eq. (13):

$$\mathbf{k}_{NL} = \int_A \sigma dA \int_L \mathbf{G}^T \otimes \mathbf{G} dx \equiv P \int_L \mathbf{G}^T \otimes \mathbf{G} dx \quad (19)$$

Here “P” is axial force on the beam. Geometrical stiffness matrix is given by the Eq. (20),

$$\mathbf{k}_G = S \begin{bmatrix} 0 & 0 & 0 & 0 & 0 & 0 \\ & \frac{c_{ij}+c_{ji}}{L^2} + \frac{1}{L} & \frac{c_{ij}}{L} & 0 & -\frac{c_{ij}+c_{ji}}{L^2} - \frac{1}{L} & \frac{c_{ji}}{L} \\ & & a_{ij} & 0 & -\frac{c_{ij}}{L} & b_{ij} \\ & & & 0 & 0 & 0 \\ & & & & \frac{c_{ij}+c_{ji}}{L^2} + \frac{1}{L} & -\frac{c_{ji}}{L} \\ sym & & & & & a_{ji} \end{bmatrix} \quad (20)$$

with coefficients:

$$\begin{aligned} a_{ij} &= \frac{p^2 L(k^2 - 3k + 6)}{30}, \\ b_{ij} = b_{ji} &= -\frac{kpL(21 - 9k - 9p + kp)}{120}, \\ a_{ji} &= \frac{k^2 L(p^2 - 3p + 6)}{30}, \\ c_{ij} = a_{ij} + b_{ij} &= \frac{p^2 L(3k^2 + k^2 p - 7k + 8p - kp)}{40}, \\ c_{ji} = a_{ji} + b_{ji} &= \frac{k^2 L(3p^2 + p^2 k - 7p + 8k - kp)}{40} \end{aligned} \quad (21)$$

The equations (18) and (20) define these matrices in the local coordinate system. Matrices in the global coordinate system are obtained by application of the transformation:

$$\mathbf{k}_{tG} = \mathbf{T}^T \cdot \mathbf{k}_t \cdot \mathbf{T}, \quad (22)$$

where \mathbf{k}_{tG} - tangent stiffness matrix in a global coordinate system and \mathbf{T} - transformation matrix.

For the plane beam, the transformation matrix \mathbf{T} is:

$$\mathbf{T} = \begin{bmatrix} \cos \alpha_c & \sin \alpha_c & 0 & 0 & 0 & 0 \\ -\sin \alpha_c & \cos \alpha_c & 0 & 0 & 0 & 0 \\ 0 & 0 & 1 & 0 & 0 & 0 \\ 0 & 0 & 0 & \cos \alpha_c & \sin \alpha_c & 0 \\ 0 & 0 & 0 & -\sin \alpha_c & \cos \alpha_c & 0 \\ 0 & 0 & 0 & 0 & 0 & 1 \end{bmatrix} \quad (23)$$

where α_c - angle between local x -axis and global X -axis for “C” configuration.

The tangent stiffness matrix of the system \mathbf{K}_t is assembled by superposition of corresponding matrices of FE, according to the criterion of system joint linking, by means of the relation:

$$\mathbf{K}_t = \sum_{i=1}^n \mathbf{Z}_i^T \cdot \mathbf{T}_i^T \cdot \mathbf{k}_{ti} \cdot \mathbf{T}_i \cdot \mathbf{Z}_i, \quad (24)$$

where \mathbf{Z}_i are matrices whose rows contain either zeroes or are equal to one at places where parameters of joint displacement of FE correspond to the joint displacement of the FE system.

7 FE Cross-section and joint forces

Incremental stresses in a beam FE can be obtained from the Eq. (12), that is:

$$\Delta\sigma_x(x, y) = E_t \Delta\varepsilon_x(x, y) = E_t \left(\mathbf{B} \cdot \Delta\mathbf{u} + \frac{1}{2} \Delta\mathbf{u}^T \cdot (\mathbf{G}^T \otimes \mathbf{G}) \cdot \Delta\mathbf{u} \right) \quad (25)$$

Forces in joints for each FE of the system are obtained from the relations:

$$\mathbf{q} = \int_V \mathbf{B}^T \sigma_t dV, \quad (26)$$

$$\mathbf{q}_i = \int_V \mathbf{B}_i \sigma dV = L \int_0^1 \mathbf{B}_i ds \int_A \sigma dA. \quad (27)$$

Normal stress is given as the function $\sigma(s, y)$ and, in general case, it has a different value for each layer of the cross-section and for each beam segment. Forces \mathbf{q}_i are obtained by numerical integration, according to the following equation:

$$\mathbf{q}_i = \sum_{g=1}^m \mathbf{B}_i(s_g) \left(\sum_{l=1}^n -y_l \sigma(l, g) A_l \right) w_g, \quad (28)$$

where

- m - number of numerical integration points,
- n - number of layers in cross-section,
- s_g - abscissa of the integration point and
- w_g - coefficient of numerical integration.

Computation of FE sections forces is carried out, before all, due to the residual load computation, what is the consequence of the non-fulfillment of equilibrium conditions in an incremental procedure.

8 Constitutive rules

For modeling of concrete and steel behavior under load, it is necessary to define constitutive rules for both materials. The following combination of models has been chosen for the constitutive model for concrete under cyclic loading (loading, unloading, and reloading):

- Hongestad's model for concrete in compression with branches of unloading/reloading, modified in the manner to involve the influence of the transversal reinforcement (stirrups),
- CEB-FIP model for tensile concrete supplemented with unloading/reloading branches, by whose shape implicitly is comprised the bond phenomenon and
- bilinear model for steel with hardening branch.

In Fig. 4 given is a diagram that defines the constitutive model for concrete and steel for cyclic loading.

The assumptions are the following:

- plastic creep (yield) of concrete in zone of compression when strain reaches the value ε_o what corresponds to the stress $\sigma_o = 0.85 \bullet f_c$,
- failure state in compression zone occurs when the strain reaches a value of limit strain ε_u ,
- appearance of cracks in concrete occurs when the strain in tensile zone reaches the value ε_{to} what corresponds to the tensile strength σ_{to} and

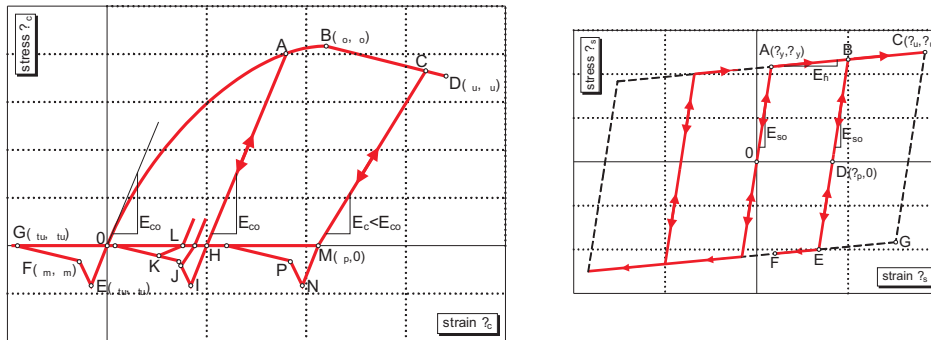


Figure 4: Adopted constitutive rule for concrete and steel for cyclic loading

- after the appearance of cracks the concrete in that zone can not receive tensile stresses, but it can receive compression stresses, after closing the cracks during the unloading.

Parameters that determine the model are:

- initial elasticity modulus of concrete for compression and tension,
- compression strength and corresponding strain,
- tensile strength and corresponding strain,
- limit strain for cracked concrete,
- “transition” and limit strain for tensile concrete and
- distance and area of transversal reinforcement.

In the diagram of proposed constitutive model the following phases are seen:

- state of compression (segment of the curve O-A-B),
- state of plastic creep (segment of the curve B-C-D),
- state of concrete crushing (behind the point D),
- state of unloading/reloading if strains have not reached the value ϵ_o (line A-H-I),

- state of unloading/reloading if strains have reached the value $\varepsilon_{co} \leq \varepsilon_o$ (segment C-M-N),
- tensile state if strains have not reached the value ε_{to} (straight line O-E),
- tensile state if strains are $\varepsilon_{to} \leq \varepsilon_t \leq \varepsilon_{tm}$ (straight line E-F),
- tensile state if strains are $\varepsilon_{tm} \leq \varepsilon_t \leq \varepsilon_{tu}$ (straight line F-G) and
- opening/closing of cracks (horizontal line from the point G).

Modification of Hognestad's model for compressed concrete, in order to include the influence of transversal reinforcement (Kent and Park, see [6]), has the form:

$$\sigma_c = \sigma_0 \alpha \left(2 - \frac{\alpha}{k}\right) \quad \text{for} \quad \varepsilon_0 \geq \varepsilon_c \geq 0, \quad (29)$$

$$\sigma_c = k\sigma_0 [1 - z(\varepsilon_c - \varepsilon_0)] \quad \text{for} \quad \varepsilon_u \geq \varepsilon_c \geq \varepsilon_0, \quad (30)$$

with

$$k = 1 + r_t \frac{\sigma_y}{\sigma_0}, \quad (31)$$

$$z = \frac{0.5}{T_1 + T_2 - 0.002k}, \quad (32)$$

$$T_1 = \frac{3 + 0.2844f_c}{14.22f_c - 1000}, \quad (33)$$

$$T_2 = 0.75r_t \sqrt{\frac{b_c}{s_t}}, \quad (34)$$

where

σ_y - stress in reinforcement at yield limit,

r_t - ratio between volume of transversal reinforcement (one stirrup) and concrete core comprised by transversal reinforcement (between two neighboring stirrups),

b_c - width of concrete core comprised by stirrups and

s_t - stirrups distance.

Limit strain of concrete with stirrups is $\varepsilon_{uc} = 0.8/z + \varepsilon_o k$. It is taken that $z = 75$ for concrete without stirrups. This modification, opposite to

many simply qualitative recommendations, enables modeling the behavior of reinforced concrete elements in cases when limit-bearing capacity (dynamic and seismic loading) is reached.

It is taken that residual strain ε_{tr} in tension zone is function of strain which is reached before start of unloading:

$$\varepsilon_{tr} = \alpha(\varepsilon_t - \varepsilon_{to}) \quad 0 \leq \alpha \leq 1 \quad (35)$$

By adoption that $\alpha = 0$ it is accepted that in tensile zone there are no residual strains, what is not a real assumption. On the other hand, it is found that by selecting the value $\alpha \geq 0.5$, that relatively large residual strain occurs, and therefore it is proposed that the value of this coefficient is $\alpha = 0.2 \sim 0.3$. By varying the coefficient α , the effects of earlier appearance of strain compression can be modeled in the zone which before unloading was exposed to tension. This is the consequence of a displacement of parts of the aggregate and cement mortar in zones of cracks and a possibility to transfer compression stress before the crack is completely closed.

In the formulation of a steel constitutive rule, the following assumptions are taken:

- steel yielding occurs when strain reaches value ε_y that corresponds to stress at yield limit ε_y ,
- state of failure in reinforcement occurs when strain reaches value of limit ε_u ,
- the envelope, within which the hysteresis process happens, has the "height" equal to double value of strains at yield limit (i.e. $2\sigma_y$) and
- characteristics of steel reinforcement are equal for tension and compression.

Parameters that determine model are:

- initial elasticity modulus of reinforcement E_{s0} ,
- stress at yield limit,
- strain at failure limit (strength of the steel) and

- hardening modulus E_h .

In the following diagram presenting the proposed constitutive model the following phases exist:

- state of compression or tension up to yield limit (segment of the curve O-A),

$$\sigma_s = E_{so}\varepsilon_s \quad \text{for} \quad \varepsilon_s \leq \varepsilon_y; \quad (36)$$

- yielding state (segments A-B-C or G-E-F),

$$\sigma_s = E_h\varepsilon_s \pm (\sigma_y - E_h\varepsilon_y) \quad \text{for} \quad \varepsilon_y \leq \varepsilon_s \leq \varepsilon_u; \quad (37)$$

- unloading/reloading state (segment B-D-E),

$$\sigma_s = E_{so}(\varepsilon_s - \varepsilon_p); \quad (38)$$

- failure state (after the point C) $\sigma_s=0$ for $\varepsilon_s \geq \varepsilon_u$.

A proposal of constitutive rule accounting for the FD change, which is compatible with tensioned concrete constitutive rule, is given in Fig. 5.

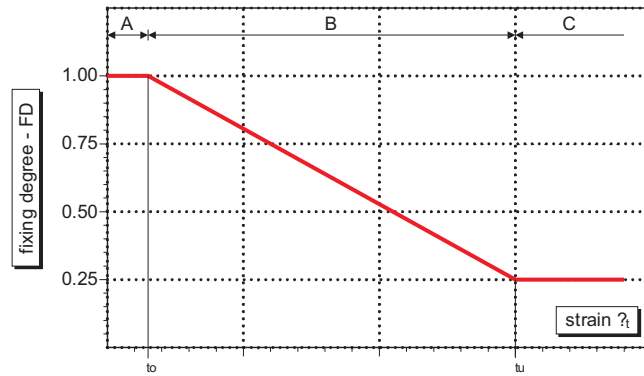


Figure 5: Joint FD change rule diagram

The following assumptions are accepted:

- FD change phenomenon is realized only for angle-jointed element (beam-column connection, for example).

- Rotational joint deterioration criterion is associated with constitutive rule for concrete in tension and depends on cracks appearance. Maximal FD value (totally fixed joint) and minimal FD value (partially fixed joint) corresponds to minimal and maximal opening of crack in tensioned beam's joint zone.
- FD change constitutive rule is the linear function and remains the same for loading, unloading and reloading state.
- Residual joint rotation does not exist (ideal unloading).

Parameters of the proposed model are:

- initial joint stiffness (i.e. starting fixing degree value, $FD_{max} = 1.0$, zone "A" of diagram),
- linear change from initial to minimal FD value (zone "B" of diagram),
- minimal FD value ($FD_{min} = 0.2 \sim 0.3$, zone "C" of diagram) which corresponds to some experimental data.

9 Proposal for inclined cracks modeling

In a presented smeared cracks layered model, the inclined cracks are modeling by appearance of appropriate "shifted" vertical cracks in layers. For large enough number of thin layers, effect of inclined cracks is attained (Fig. 6). Criterion of appearance of these "shifted" vertical cracks is a reaching of the limit tension stress in concrete, caused by simultaneous action of normal (axial) and shear stresses.

Therefore, it is very important to compute properly the cross-sectional and a whole beam FE stiffness parameters.

Relation between principal stress and, at the other hand, axial and shear stress is well known:

$$\sigma_{\alpha i} = \frac{\sigma_{xi}}{2} \pm \sqrt{\frac{\sigma_{xi}^2}{4} + \tau_i}, \quad \alpha \in \{1, 2\}. \quad (39)$$

where in i^{th} layer:

$\sigma_{\alpha i}$ - are the principal stresses,
 σ_{xi} - axial (normal) stress and
 τ_i - shear stress.

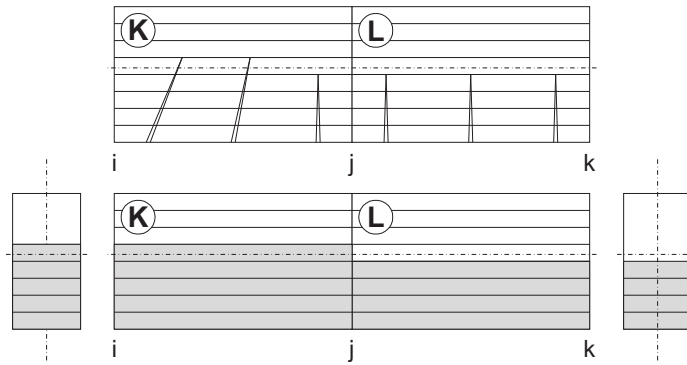


Figure 6: “Smearred cracks approach” in inclined cracks modeling

Computation of the axial stress σ_{xi} is based on “ $\sigma - \varepsilon$ ” concrete constitutive rule, and shear stress is computed according to expression:

$$\tau_i = \frac{TS_i}{Ib_i} \quad (40)$$

where

T - shear force,

S_i - moment of area of layers above of the i^{th} layer,

I - cross-section moment of inertia and

b_i - width of i^{th} layer.

In contrast to procedures based on design code (Fig. 7 a-b), computation of “ T ” and “ S_i ” in the proposed model is performed for the whole cross-section (Fig. 7c) regardless of the stress-strain state due to manifestation of “secondary” way of force transfer (“aggregate interlock shear transfer”, “dowel action shear transfer”, etc.).

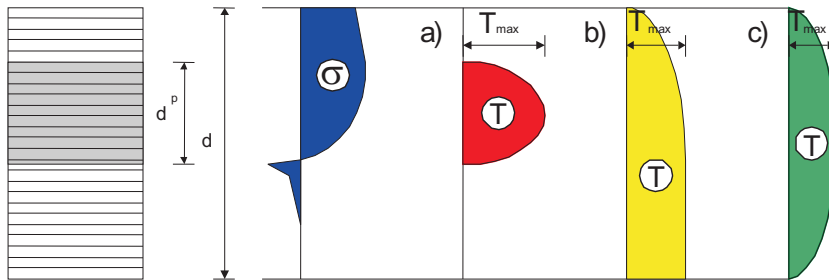


Figure 7: Various approaches in shear area computation

10 Beam FE and cross-section stiffness

Layered approach makes possible a monitoring of the stress-strain state and the determination of stiffness and bearing capacity both for cross-section and for the beam FE in the whole. As significant, the questions of discretization method are pointed out here, i.e.:

- adoption of optimum number of beam FE for division of beams of a structural system,
- adoption of optimum number of integration points within one beam FE and
- adoption of optimum number of layers within the cross-section of the beam FE.

The function of error distribution indicates that the optimum number of FE along the beam structural element has to be between four and eight. The establishment of rougher division (less than 4 FE per beam) contributes to a certain increase of efficiency analysis, but also to a considerable increase of approximation error. Increase of a number of FE along the beam of the system (10 and more) does not contribute to the essential increase of accuracy, but considerably degrades numerical efficiency of analysis.

The stiffness matrix coefficient of beam FE can be obtained by application of any numerical integration methods. Usually the Gauss numerical integration scheme is adopted.

If a sufficient number of beam FE is adopted, a sufficient accuracy can be achieved even in the case of integration scheme with a small number of integration points. In order to satisfy conditions of numerical efficiency and to provide a sufficient accuracy, the integration scheme with three Gauss' points has been chosen here. In Fig. 8 positions of Gauss points are displayed with coefficients of integration for a beam FE divided into layers along the height.

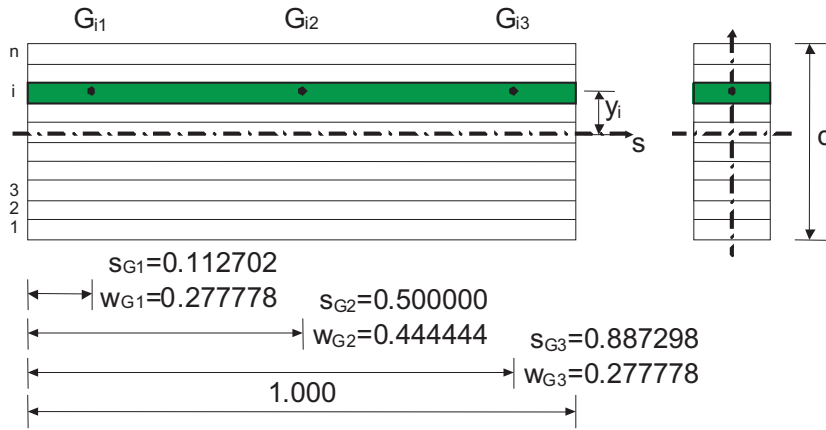


Figure 8: Three point Gauss integration scheme

As already emphasized, the constant value of tangent modulus in one layer along the FE length has been adopted. Namely, it can be accepted that stiffness and bearing capacity of the element, in the section corresponding to a middle Gauss' point, is valid for whole length of the finite element. This should not significantly jeopardize the solution accuracy, taking into consideration the nature of iterative method applied for residual loading balancing (standard and modified Newton-Raphson's method).

The equation that defines coefficients of elastic-plastic stiffness matrix now has the following form:

$$\mathbf{k}_L = \int_A E_t dA \int_L \mathbf{B}^T \otimes \mathbf{B} dx = \sum_{i=1}^n E_t dA \int_L \mathbf{B}^T \otimes \mathbf{B} dx. \quad (41)$$

The first integral depends on characteristics of the cross-section, while the second one is a function of the beam's axis. Differently from standard approach, where a constant value of the modulus in one layer is assumed, here a change of tangent modulus is adopted that corresponds to a selected constitutive rule for concrete (Fig. 9).

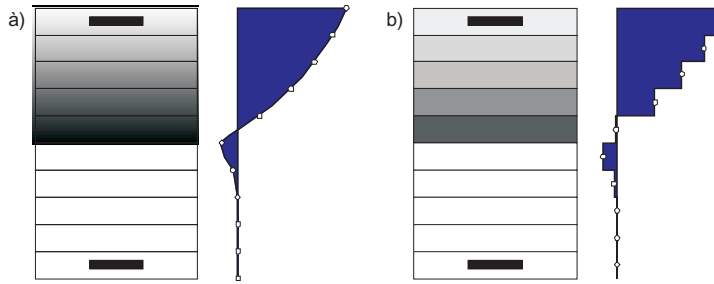


Figure 9: Stress and tangent modulus distribution in cross-section

Adoption of continuously variable stiffness along the layer height (Fig. 9a) contributes to an increase of the computational accuracy of the cross-section overall stiffness in relation to the standard method (Fig. 9b). A force that corresponds to one layer is defined by taking the parabolic distribution of stresses. The parabola within one layer is obtained as a segment of the parabola for two neighboring layers. Such type of numerical integration corresponds to a well-known finite difference method.

Application of the method formulated in such a way will not have any considerable increase of complexity and computation time for the consequence. According to the numerical tests presented in [3], a cross-section stiffness calculation, FE stiffness calculation and assembling of FE system stiffness matrix do not participate highly in the total computation time (approx. 5% for medium-scale systems and 2% for large-scale FE systems).

Equations, which define cross-section stiffness, remain formally the same:

$$EA = \int_A E_t dA = \sum_{i=1}^{nc} E_{ti} A_i + \sum_{j=1}^{ns} E_{tj} A_j \quad (42)$$

$$ES = \int_A y E_t dA = \sum_{i=1}^{nc} y_i E_{ti} A_i + \sum_{j=1}^{ns} y_j E_{tj} A_j \quad (43)$$

$$EI = \int_A y^2 E_t dA = \sum_{i=1}^{nc} y_i^2 E_{ti} A_i + \sum_{j=1}^{ns} y_j^2 E_{tj} A_j \quad (44)$$

where are:

y_i - distance of the center of gravity of the trapezoidal area from the referent axis and

y_j - distance of the center of the reinforcement layer from the referent axis of the section.

The total number of layers of concrete and reinforcement is “ nc ” and “ ns ” respectively.

Only three forces are independent (axial force and two moments at the beam’s ends), while the other three forces are determined from the equilibrium conditions. Equations for the independent forces are:

$$N = \int_A \sigma dA = \sum_{i=1}^{nc} \sigma_{ci} A_i + \sum_{j=1}^{ns} \sigma_{sj} A_j, \quad (45)$$

$$M = \int_A \sigma y dA = \sum_{i=1}^{nc} \sigma_{ci} y_i A_i + \sum_{j=1}^{ns} \sigma_{sj} y_j A_j. \quad (46)$$

Based on preliminary research it can be concluded that the optimum layer’s height is between 5% and 10% of the cross-section height. If the layers have the same thickness (what is justifiable in majority of cases), the optimum number of layers is between 10 and 20. By application of the standard method, with a few layers (4 – 6), the satisfactory results can be obtained, just in the case of loading of around 50% of the limit one. In addition, small number of layers may be applied in the case of a state of stresses close to the homogenous one (relatively great axial force of compression or tension combined with relatively small moment).

In case of monotonic loading without unloading (what is, in fact, very rare case) with application of one “non-incremental” method (computing of total stresses on the basis of total strain in a layer), the minimum error would be obtained even without division of the cross-section into layers.

Existence of at least one cycle of unloading/reloading or cyclic loading requires the application of incremental method (computing of total stresses based on stresses from the previous configuration and increments of stresses from the current configuration of the system). During that, division into a greater number of layers solves the problem of a more accurate including of the previous history of loading influence (residual deformations and stresses, first of all).

Additional increase of number of layers (over 20) does not contribute to essential improvement of the accuracy, consequently the “limit” of 20 layers can be observed as the upper optimum.

11 Numerical tests

As an illustration of previous propositions, the results of the numerical tests - one linear and three nonlinear analysis of one simple reinforced concrete frame loaded by three seismic actions are presented. Seismic loading is selected for numerical tests because in the case of simple static monotonic loading advantages of proposed model are not enough expressed (as is shown in [4]).

Beam FE mass matrix is composed as diagonal (lumped mass model), where the influence of rotational inertia is neglected. Damping matrix of structure is composed to be proportional to initial stiffness matrix. Such an approach is used because the hysteresis dissipation effects (consequences of material nonlinearity - appearance of cracks, crushing of concrete in compressed zone and yield of reinforcement) in nonlinear systems, are dominant opposite to viscous damping effects, which are expressed in linear systems.

For numerical integration of dynamic equilibrium, Eq. (47) , the Newmark integration procedure (with increment $\Delta t = 5ms$) is applied as well as a modified Newton-Raphson iterative procedure for balancing the residual loads:

$$\mathbf{M} \cdot \ddot{\mathbf{u}} + \mathbf{C} \cdot \dot{\mathbf{u}} + \mathbf{K}_t \cdot \mathbf{u} = -\mathbf{M} \cdot \ddot{\mathbf{u}}_g, \quad (47)$$

where

\mathbf{M} - mass matrix of the system,
 \mathbf{C} - the system damping matrix,
 \mathbf{K}_t - the system tangent stiffness matrix and
 $\{\ddot{u}\}$, $\{\dot{u}\}$, $\{u\}$, $\{\ddot{u}_g\}$ –vectors of acceleration, velocity, displacement and ground acceleration.

The adoption of Newmark numerical integration procedure is reasonable due to its own stability and convergence, Fig. 10.

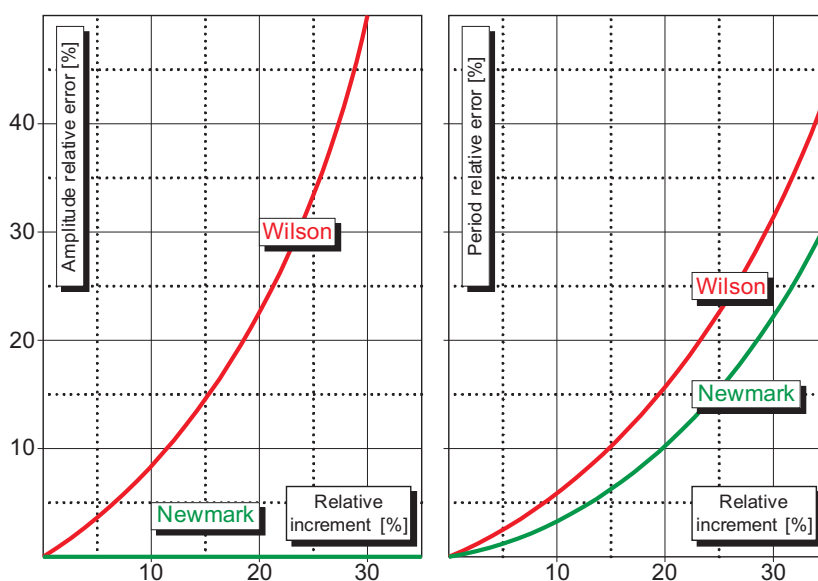


Figure 10: Willson vs. Newmark comparison of amplitude/periode relative error

Modified Newton-Raphson (MNR) iterative procedure is adopted because the numerical efficiency and accuracy in regard to its standard form (NR), secant and Broyden-Fletcher-Goldfarb-Shano (BFGS) methods, Fig. 11.

Fig. 12 illustrates beam FE system (48 joints, 48 beams), mass distribution ($m_i = 400kg$), geometrical and mechanical characteristics (moduli $E_c = 31.5 GPa$, $E_s = 210 GPa$ and viscous damping $\mu = 0.05$) of RC frame.

Following seismic excitations (accelerograms in the Fig. 13–15) are used in numerical tests:

- San Fernando (20 s record Ventura, 1971),

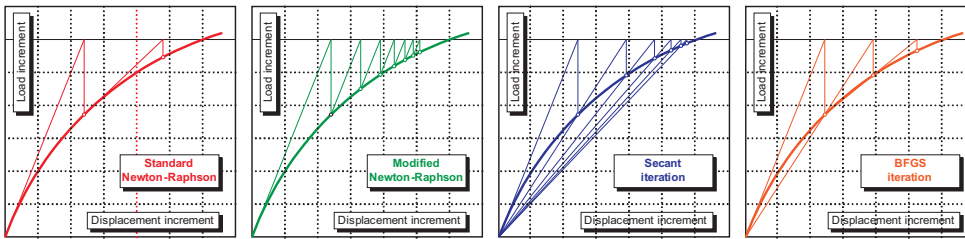


Figure 11: Comparison of MNR with other iterative methods

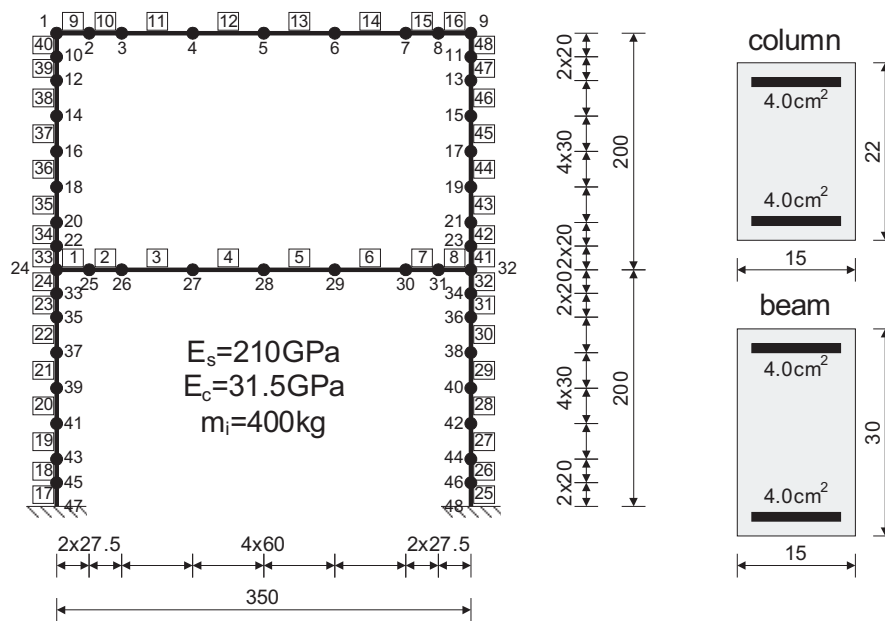


Figure 12: Beam FE model of analyzed RC frame

- Parkfield (20 s record Temblor, 1966) and
- Imperial Valley (20 s record El Centro, 1940).

All three seismic actions have different magnitude value and frequency configuration as well as different form of “main stroke” zone. Therefore for each of them the diverse energy amount enters into the structure, which is evident from the structural behavior. Simply “large magnitude value” or only “malign frequency range” are not the sufficient

reasons for large structural excitation. Appropriate time combination of seismic magnitude and seismic frequency characteristic make the main and real difference between various seismic actions.

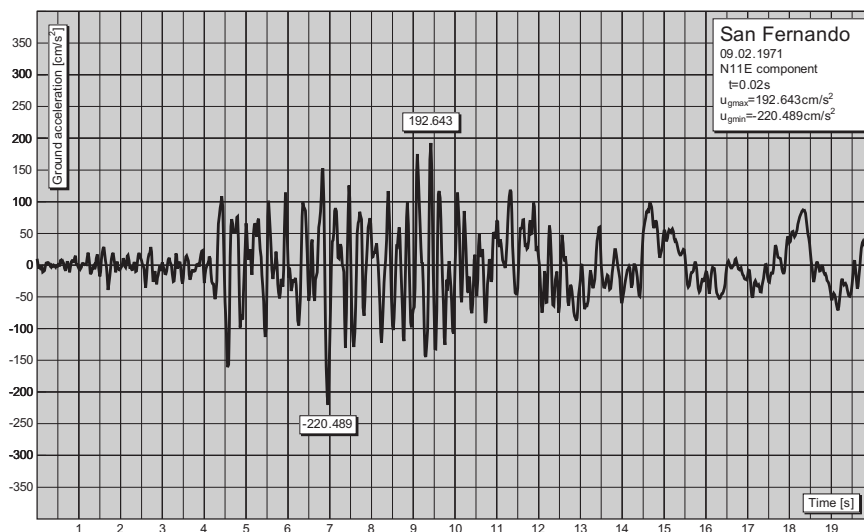


Figure 13: San Fernando earthquake accelerogram (Ventura Blvd. record)

For each seismic action the following analysis are performed:

- linear “L” analysis,
- geometric nonlinear “G” analysis,
- simultaneous (geometric & material) nonlinear “MG” analysis,
- simultaneous nonlinear analysis “MGS” with modeling of inclined cracks and
- simultaneous nonlinear analysis “MGC” with modeling of joint deterioration.

In the Figures 16–18 the diagrams of a time history of a RC frame displacement are presented.

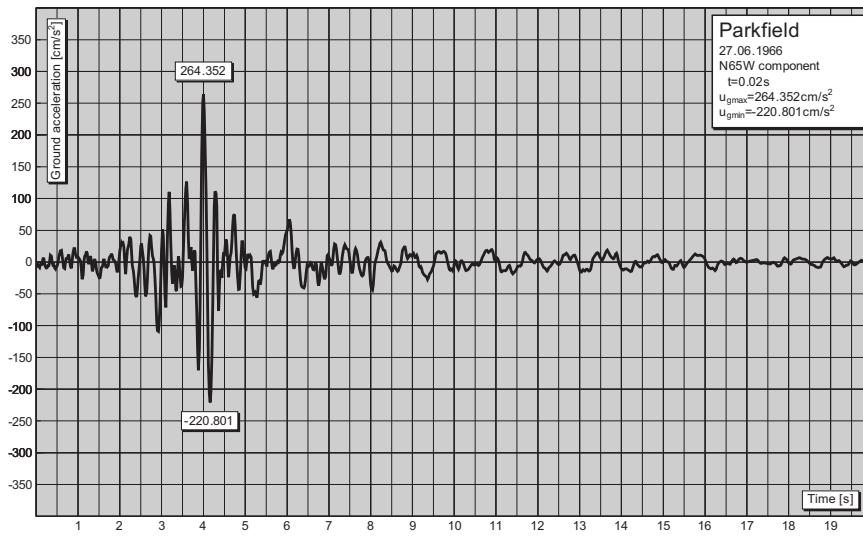


Figure 14: Parkfield earthquake accelerogram (Temblor record)

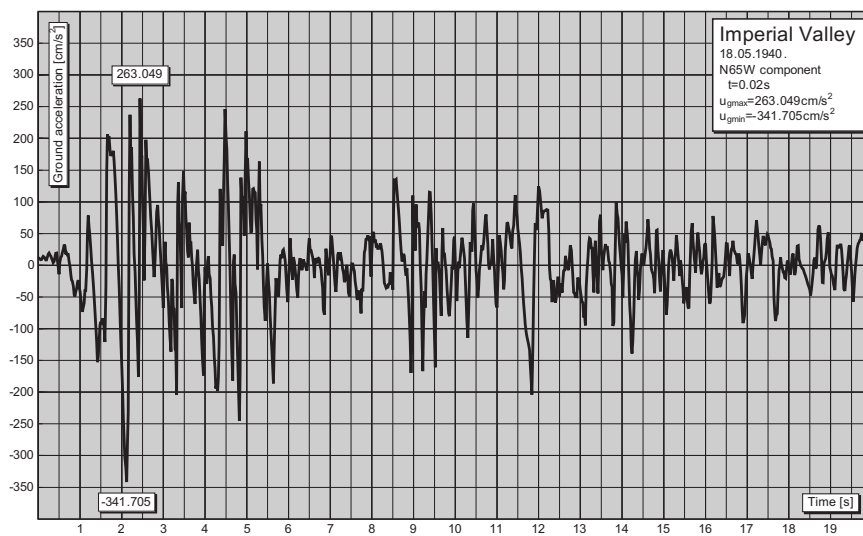


Figure 15: Imperial Valley earthquake accelerogram (El Centro record)

Not only the proportion between displacement response values, but in some cases, completely different behavior of RC frame model is substantial, especially for a strong seismic excitation.

Differences between results for “L” analysis and anyone of performed nonlinear analysis indicate the justification of nonlinear model usage, except of “G” analysis. Namely, because of a comparatively small horizontal displacement and small vertical loads, for this testing of RC frame, the geometric nonlinear effects are not significant. Therefore, the results of “G” analysis are not given in comparison with others.

On the other hand, the “MGS” analysis results are skipped as negligible additional nonlinear effects to effects of simultaneous nonlinearity (“MG” analysis).

12 Conclusions

Proposed numerical concept for simulation of structural behavior of RC frames loaded by seismic forces is formulated as a compromise solution. Compromise is made between the accuracy, as an essential parameter, and, on the other hand, simplicity, as everyday design practice task. The objective of presented research was to find an optimal way using nonlinear analysis of mentioned structures.

Opposite to the complex 2D and 3D FE models, mostly used in theoretical consideration, the reasonably simple model is proposed. The suggested model is based on 2D beam FE with abilities characteristic for more sophisticated models. Opposite to standard beam FE models, that include only the concrete and reinforcement behavior modeling, suggested 2D beam FE model considers frame joint deterioration as well as interaction of shear and flexural forces.

The final verification and implementation of this modeling concept is proved by means of the parametric test analysis i.e. in comparison with the experimental data and results obtained by application of some complex model. It is direction of future research on this modeling concept.

Acknowledgement

This paper is a presentation of research performed within the Scientific Project *N^o 6517 A* granted by the Ministry of Science and Environmental Protection of the Republic of Serbia.

References

- [1] Blaauwendraad, J. & De Groot, A.K: Progress in Research on Reinforced Concrete Plane Frames, HERON, Vol. 28, No. 2, Delft, (1983).
- [2] Burns, N.H., & Siess, C.P: Repeated and Reversed Loading in Reinforced Concrete, Journal of the Structural Division, ASCE, Vol. 92, No. 5, (1966) New York, 65-78.
- [3] D. Kovačević: Numerical modeling of Behaviour of Reinforced Concrete Frames Loaded by Seismic Actions, Ph.D. Thesis, Civil Engineering Faculty, University of Belgrade, 2001.
- [4] M. Sekulović, D.Milašinović and D. Kovačević: Increasing of Numerical Efficiency in Nonlinear Analysis of Reinforced Concrete Beam Elements, CST '96 - 3rd International Conference on Computational Structures Technology, Ed. B.H.V. Topping, Civil-Comp. Press, Meigle Printers, Scotland, (1996), pp.139-150.
- [5] Scordelis, A : Computers Models for Nonlinear Analysis of Reinforced and Prestressed Concrete Structures, PCI Journal, N° 11-12, (1984), 116-135.
- [6] Behavior and Analysis of Reinforced Concrete Structures under Alternate Actions Inducing Inelastic Response, Vol. 1: General Models, CEB Bulletin d'information N° 210, Lausanne, (1991)
- [7] Semi-rigid Structural Connections , IABSE Colloquium Report, Istanbul, (1996).

Submitted on May 2005, revised on November 2005.

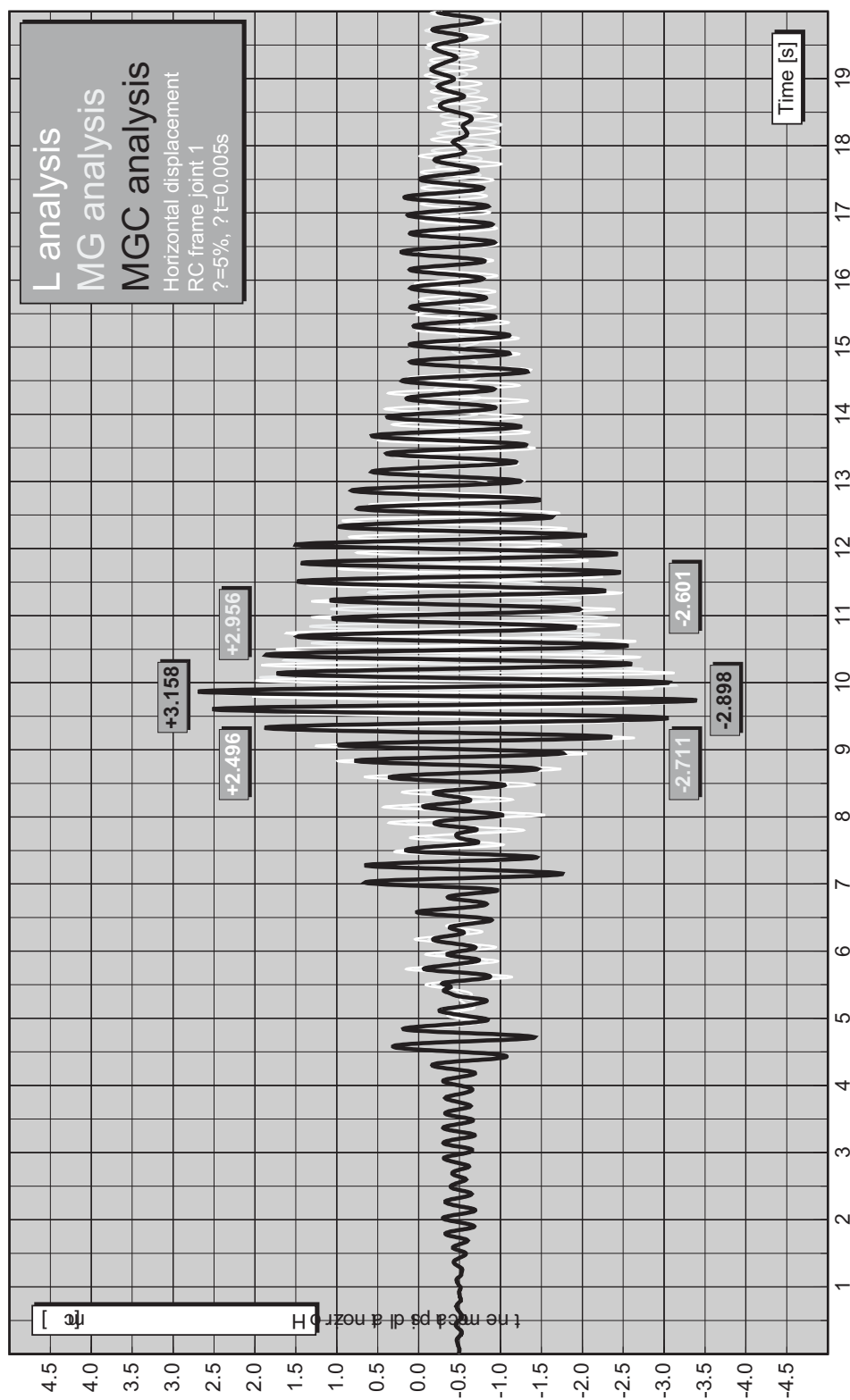


Figure 16: Displacement time history of RC frame (San Fernando earthquake)

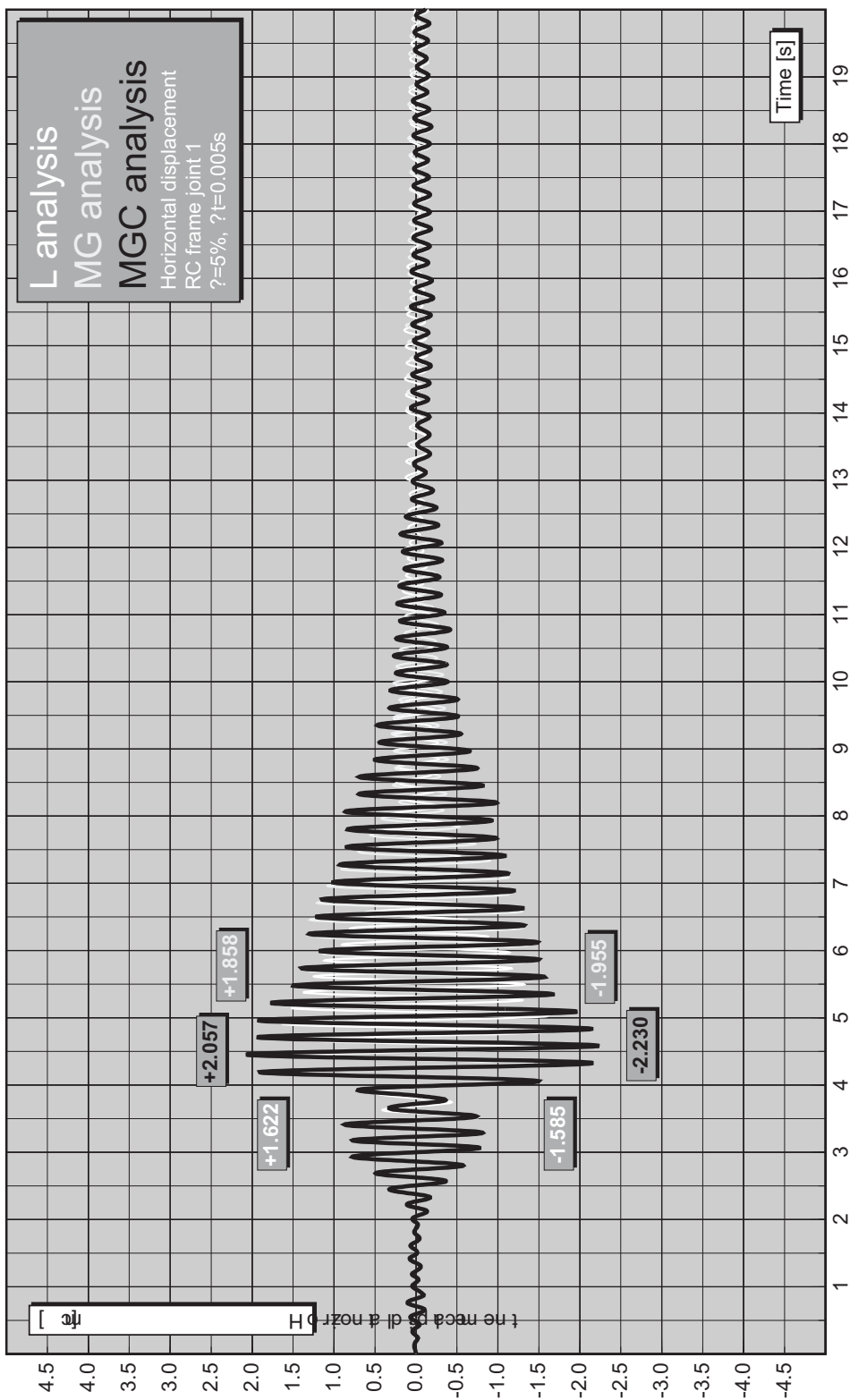


Figure 17: Displacement time history of RC frame (Parkfield earthquake)

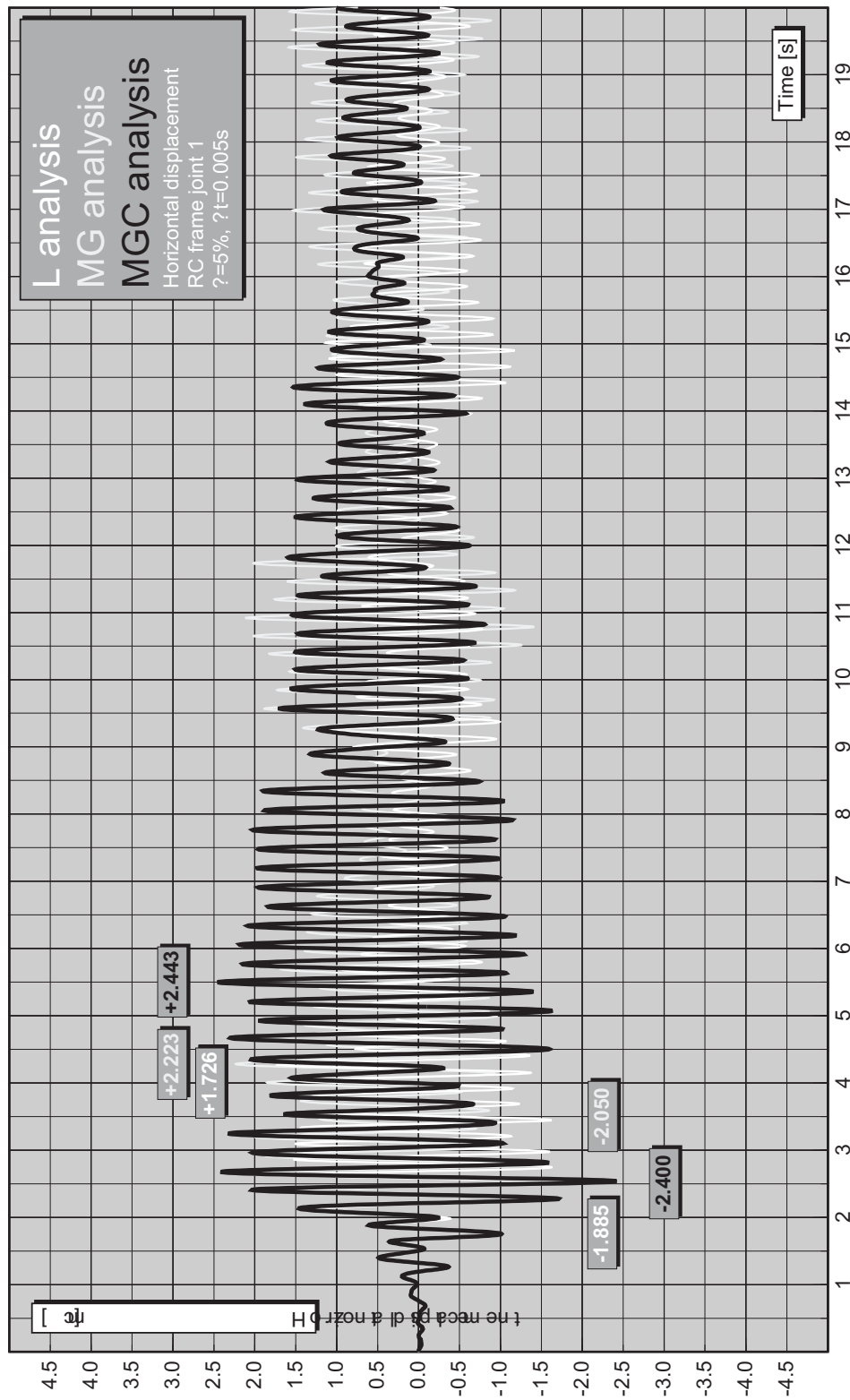


Figure 18: Displacement time history of RC frame (Imperial Valley earthquake)

MKE model za armiranobetonske okvire opterećene seizmičkim silama

UDK 536.7

Cilj prikazanih istraživanja je formulisanje dovoljno sofisticiranog i za inženjersku praksu, pogodnog MKE numeričkog modela za armiranobetonske okvire opterećene seizmičkim dejstvima. Za modeliranje betona i čelika primenjeni su radni dijagrami za jednoosno stanje napona. Pored toga dat je predlog modela za obuhvatanje uticaja popustljivosti čvorova, kao i uticaja interakcije smičucih i normalnih napona (efekat kosih prslina). Rezultati nekoliko numeričkih testova (linerni/nelinearna analiza armiranobetonskog okvira za tri seizmička dejstva) dati su kao ilustracija prikazanih teorijskih istraživanja.